GLOBAL BIOGEOCHEMICAL CYCLES, VOL. 20, GB4013, doi:10.1029/2005GB002676, 2006

Large accumulation of anthropogenic CO_2 in the East (Japan) Sea and its significant impact on carbonate chemistry

Geun-Ha Park,[1] Kitack Lee,[1] Pavel Tishchenko,[2] Dong-Ha Min,[3] Mark J. Warner,[4] Lynne D. Talley,[5] Dong-Jin Kang,[6] and Kyung-Ryul Kim[6]

Received 19 December 2005; revised 10 July 2006; accepted 26 July 2006; published 22 November 2006.

[1]   This paper reports on a basin-wide inventory of anthropogenic CO_2 in the East (Japan) Sea determined from high-quality alkalinity, chlorofluorocarbon, and nutrient data collected during a summertime survey in 1999 and total dissolved inorganic carbon data calculated from pH and alkalinity measurements. The data set comprises measurements from 203 hydrographic stations and covers most of the East Sea with the exception of the northwestern boundary region. Anthropogenic CO_2 concentrations are estimated by separating this value from total dissolved inorganic carbon using a tracer-based (chlorofluorocarbon) separation technique. Wintertime surface CFC-12 data collected in regions of deep water formation off Vladivostok, Russia, improve the accuracy of estimates of anthropogenic CO_2 concentrations by providing improved air-sea CO_2 disequilibrium values for intermediate and deep waters. Our calculation yields a total anthropogenic CO_2 inventory in the East Sea of 0.40 ± 0.06 petagrams of carbon as of 1999. Anthropogenic CO_2 has already reached the bottom of the East Sea, largely owing to the effective transport of anthropogenic CO_2 from the surface to the ocean interior via deep water formation in the waters off Vladivostok. The highest specific column inventory (vertically integrated inventory per square meter) of anthropogenic CO_2 of 80 mol C m^{-2} is found in the Japan Basin ($40°N-44°N$). Comparison of this inventory with those for other major basins of the same latitude band reveal that the East Sea values are much higher than the inventory for the Pacific Ocean ($20-30$ mol C m^{-2}) and are similar to the inventory for the North Atlantic ($66-72$ mol C m^{-2}). The substantial accumulation of anthropogenic CO_2 in the East Sea during the industrial era has caused the aragonite and calcite saturation horizons to move upward by $80-220$ m and $500-700$ m, respectively. These upward movements are approximately 5 times greater than those found in the North Pacific. Both the large accumulation of anthropogenic CO_2 and its significant impact on carbonate chemistry in the East Sea suggest that this sea is an important site for monitoring the future impact of the oceanic invasion of anthropogenic CO_2.

Citation: Park, G.-H., K. Lee, P. Tishchenko, D.-H. Min, M. J. Warner, L. D. Talley, D.-J. Kang, and K.-R. Kim (2006), Large accumulation of anthropogenic CO_2 in the East (Japan) Sea and its significant impact on carbonate chemistry, *Global Biogeochem. Cycles*, *20*, GB4013, doi:10.1029/2005GB002676.

[1]School of Environmental Science and Engineering, Pohang University of Science and Technology, Pohang, Korea.
[2]Pacific Oceanological Institute, Far East Division, Russian Academy of Sciences, Vladivostok, Russia.
[3]Marine Science Institute, University of Texas at Austin, Port Aransas, Texas, USA.
[4]School of Oceanography, University of Washington, Seattle, Washington, USA.
[5]Scripps Institution of Oceanography, University of California, San Diego, La Jolla, California, USA.
[6]Research Institute of Oceanography, School of Earth and Environmental Sciences (BK21), Seoul National University, Seoul, South Korea.

Copyright 2006 by the American Geophysical Union.
0886-6236/06/2005GB002676

1. Introduction

[2]   Coastal and marginal seas potentially play an important role in absorbing atmospheric CO_2 because high inputs and an efficient use of nutrients from adjoining land result in a decrease in the surface water CO_2 concentration, which in turn drives CO_2 transfer from the atmosphere to the surface ocean. These seas also play a key role in the global carbon cycle by connecting terrestrial and oceanic carbon reservoirs [*Tsunogai et al.*, 1999; *Thomas et al.*, 2004]. Little attention has been devoted to the role of coastal and marginal seas as a sink of atmospheric CO_2 because these seas account for only 7% of the total area of the world ocean. As a result, only limited information is available regarding the amount of anthropogenic CO_2 stored in coastal and marginal seas and
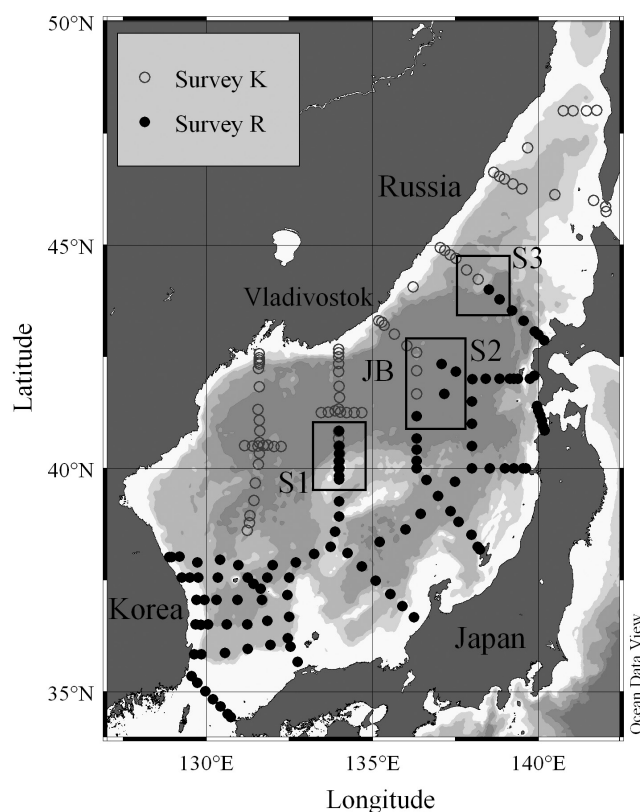
Figure 1. Shaded topography map of the East Sea showing measurements sites. Data were collected by the Circulation Research of East Asian Marginal Seas project and U.S. Office of Naval Research's Japan/East Sea Program from 24 June to 11 August 1999. Open circles represent sampling locations of Survey K conducted on the Russia *R/V Khromov*, while solid circles are sampling locations of Survey R conducted on the U.S. *R/V Roger Revelle*. JB indicates the Japan Basin. The three rectangular areas (S1−3) are discussed in Figure 2.

the mechanisms that underlie the transfer of atmospheric CO$_2$ to coastal and marginal seas and subsequently on to the open ocean.

[3] The East Sea is a marginal sea surrounded by Korea, Japan, and Russia, and is connected to the North Pacific via three straits with depths of less than 150 m. In early studies of the East Sea, Japanese investigators put forward the idea that waters deeper than ∼300 m in this sea have uniform physical and chemical characteristics. This uniform water body was originally referred to as the Proper Water [*Uda*, 1934]; however, more recent investigations have revealed that this uniform water body can be further divided into three water masses, referred to as Central Water, Deep Water, and Bottom Water [*Kim et al.*, 1996; *Kim and Kim*, 1996]. A key physical feature of the East Sea is deep water formation at the continental shelf and slope off Vladivostok, Russia [*Senjyu and Sudo*, 1993; *Kawamura and Wu*, 1998; *Kim et al.*, 2002; *Talley et al.*, 2003]. Another unique feature of the East Sea is weak vertical stability compared to that in the open ocean; for example,

vertical variations in temperature and salinity found in the East Sea below the seasonal thermocline are one to two orders of magnitude smaller than those typically found in the Pacific Ocean [*Kim and Kim*, 1996; *Kim et al.*, 2001, 2002]. Both the deep water formation and weak vertical stability found in the East Sea lead to the formation of an active deep-convection system that vigorously transfers surface water loaded with anthropogenic CO$_2$ to the interior of the basin. On the basis of the features described above, the East Sea is potentially a significant reservoir for anthropogenic CO$_2$.

[4] To verify this possibility, we applied a tracer-based separation technique [*Gruber et al.*, 1996] to CO$_2$ survey data collected from the East Sea. In the present paper, we report the basin-scale distribution of anthropogenic CO$_2$ in the East Sea and the effect of oceanic uptake of anthropogenic CO$_2$ on the saturation state of seawater with respect to biogenic calcium carbonate (CaCO$_3$) particles.

2. Data and Calculation Methods

2.1. Survey Data

[5] The data used in the present study provide a dense coverage of the East Sea and were collected from 24 June to 11 August 1999 as part of the Circulation Research of East Asian Marginal Seas project and the U.S. Office of Naval Research's Japan/East Sea Program. This field survey was jointly conducted by a multinational team of investigators from United States, Russia, and Korea. In the southern part of the East Sea, the survey (hereafter referred to as "Survey R") was conducted on the U.S. *R/V Roger Revelle*, whereas in the northern part of the sea (referred to hereafter as "Survey K") was carried out by Russian scientists on the Russia *R/V Professor Khromov* (Figure 1). A total of 203 hydrographic stations were established [*Talley et al.*, 2004]. Salinity, temperature, and nutrient concentrations were measured in all discrete samples, whereas concentrations of chlorofluorocarbons (CFC-11, CFC-12, and CFC-113) were determined in seawater samples collected from 110 of the 112 Survey R stations and 36 of the 91 Survey K stations. The precision of the chlorofluorocarbon measurements was about 0.005 pmol kg^{-1} [*Min and Warner*, 2005].

[6] Total alkalinity (A$_T$) and potentiometric pH were measured in nearly all discrete samples. The A$_T$ analysis followed Bruevich's method, which utilizes colorimetric titration by hydrochloric acid in an open system using a mixed indicator (methylene blue and methyl red) [*Bruevich*, 1944]. The titrant concentration was monitored daily by titrating certified reference materials with known values of A$_T$ and total dissolved inorganic carbon (C$_T$) (prepared and certified by A. Dickson of Scripps Institution of Oceanography, San Diego, California). The pH measurements were performed at 25°C in a potential cell without a liquid junction [*Tishchenko et al.*, 2001] and reported on the total scale, which considers the interaction of hydrogen ions with bisulfate ions [*Hansson*, 1973; *Dickson*, 1984]. To calculate C$_T$ from A$_T$ and pH measurements using the thermodynamic models, all pH values on the total hydro-

gen scale (pH_T) were converted to the seawater scale (pH_{SWS}) to be consistent with published dissociation constants of carbonic acid. The two scales are linked by the following equation:

$$pH_{SWS} = pH_T - \log\left\{\left(1 + [SO_4^{2-}]_T / K_{HSO4} + [F]_T / K_{HF}\right) / \left(1 + [SO_4^{2-}]_T / K_{HSO4}\right)\right\}, \quad (1)$$

where $[SO_4^{2-}]$ and $[F]_T$ are the total concentrations of sulfate and fluoride in seawater, respectively, and K_{HSO4} and K_{HF} are the dissociation constants of sulfate and hydrogen fluoride in seawater, respectively [*Dickson and Riley*, 1979].

[7] The measurement precisions were approximately ±4 μmol kg^{-1} for A_T and ±0.004 units for pH [*Talley et al.*, 2004]. The values of C_T used in the calculation of anthropogenic CO_2 concentration were calculated from A_T and pH measurements using the carbonic acid dissociation constants of *Mehrbach et al.* [1973] as refitted by *Dickson and Millero* [1987]. This set of carbonic acid dissociation constants provides the best correlation with global carbon measurements [*Lee et al.*, 2000; *Millero et al.*, 2002]; however, *Talley et al.* [2004] raised the concern that pH values used in the calculation of C_T may be biased by as much as 0.035 in pH. This bias was found to be the maximum difference in a comparison of two different pH measurement techniques (potentiometry versus spectrophotometry) applied to the same set of samples collected during the cruise. According to a comparison study, such a contrast in the two different pH data sets largely reflects unnecessary measurement steps associated with the spectrophotometric pH method (see auxiliary material[1]). These extra measurement steps were not included in the potentiometric pH measurement protocol. When these unnecessary steps are eliminated from the spectrophotometric measurement procedure, spectrophotometric pH values are in better agreement with potentiometric pH values. Therefore potentiometric pH values are sufficiently accurate to enable the calculation of C_T. The accuracy of the pH values is addressed in detail in the auxiliary material.

2.2. Systematic Differences in the Values of Carbon Parameters Measured During the Two Cruises

[8] We compared hydrographic and carbon parameter data obtained during Surveys R and K to assess systematic discrepancies between the two surveys. Three regions (labeled S1, S2, and S3 in Figure 1) for which the two surveys either overlap or collected data at proximate locations were arbitrarily chosen for comparison of the two data sets. Each of the three parameters, A_T, C_T, and pH, was plotted against potential density (σ_θ) for each of the three overlapping or proximal regions (Figure 2). Comparisons of the two sets of survey data from each overlapping or proximal region were undertaken by fitting the data for $\sigma_\theta > 27.2$ from each survey with a second-order polynomial function and then examining the differences between the

two curve fits (Figure 2). This method has been used previously to define systematic errors in global CO_2 survey data [*Lamb et al.*, 2002; *Sabine et al.*, 2005]. Systematic differences in measured parameters between the two data sets for the three overlap regions are summarized in Table 1. Differences in salinity (S), potential temperature (θ), oxygen concentration (O_2), and A_T are within measurement uncertainties and thus no corrections were applied to these data; however, the calculated C_T values for Survey K are 4.3 μmol kg^{-1} higher than those for Survey R. This systematic discrepancy is likely to reflect the mean pH difference of 0.014 between the two surveys. To correct for this difference in C_T, 4.3 μmol kg^{-1} was subtracted from the C_T values calculated for Survey K.

2.3. Calculation of Anthropogenic CO_2

[9] The concentration of anthropogenic CO_2 within a given parcel of water was determined using a modified version of the ΔC^* approach developed by *Gruber et al.* [1996]. Modification includes the use of an optimum multiparameter (OMP) analysis to more accurately determine the net air-sea disequilibrium for a given sample [*Sabine et al.*, 2002; *Lee et al.*, 2003]. In this method, anthropogenic CO_2 (C^{ANT}) is separated out from C_T (C_T^{CAL}; calculated from measured pH and A_T values using a thermodynamic model) via the following equation:

$$C^{ANT} = C_T^{CAL} - C_T^{EQ} - \Delta C^{BIO} - \Delta C^{DISEQ}, \quad (2)$$

where C_T^{EQ} is the total dissolved inorganic carbon in equilibrium with the preindustrial atmospheric CO_2 of 280 μatm for the sample's potential temperature, salinity, and preformed total alkalinity (A_T^o), where A_T^o represents the total alkalinity of a water parcel when it was last at the ocean surface; ΔC^{BIO} is the change in total dissolved inorganic carbon resulting from the oxidation of organic matter and dissolution of calcium carbonate, which can be estimated from changes in apparent oxygen utilization (saturation O_2 − measured O_2) and the difference between A_T and A_T^o, respectively; and ΔC^{DISEQ} is the total dissolved inorganic carbon arising from disequilibrium of the fugacity of CO_2 (fCO_2) between the atmosphere and ocean.

[10] The A_T^o values of subsurface samples were estimated from multilinear regression using salinity and NO (NO = O_2 − $R_{O2:N} \times$ N) [*Broecker*, 1974]. We chose an $R_{O2:N}$ of −10.625, as given by *Anderson and Sarmiento* [1994]. An empirical equation for A_T^o was derived using surface water A_T data, including wintertime measurements (n = 1,177) (<100 dbars),

$$A_T^o \left(\mu mol\, kg^{-1}\right) = 765.5 + 43.77 \times S + 0.03147 \times NO. \quad (3)$$

The standard deviation (1σ) of the A_T^o value estimated using equation (3) is ±6.3 μmol kg^{-1}. We found that summer-winter differences in A_T are statistically insignificant.

[11] The value of C_T^{EQ} was calculated from the A_T^o estimated from equation (3) and fCO_2 = 280 μatm using the carbonic acid dissociation constants of *Mehrbach et al.* [1973], as refitted by *Dickson and Millero* [1987]. The
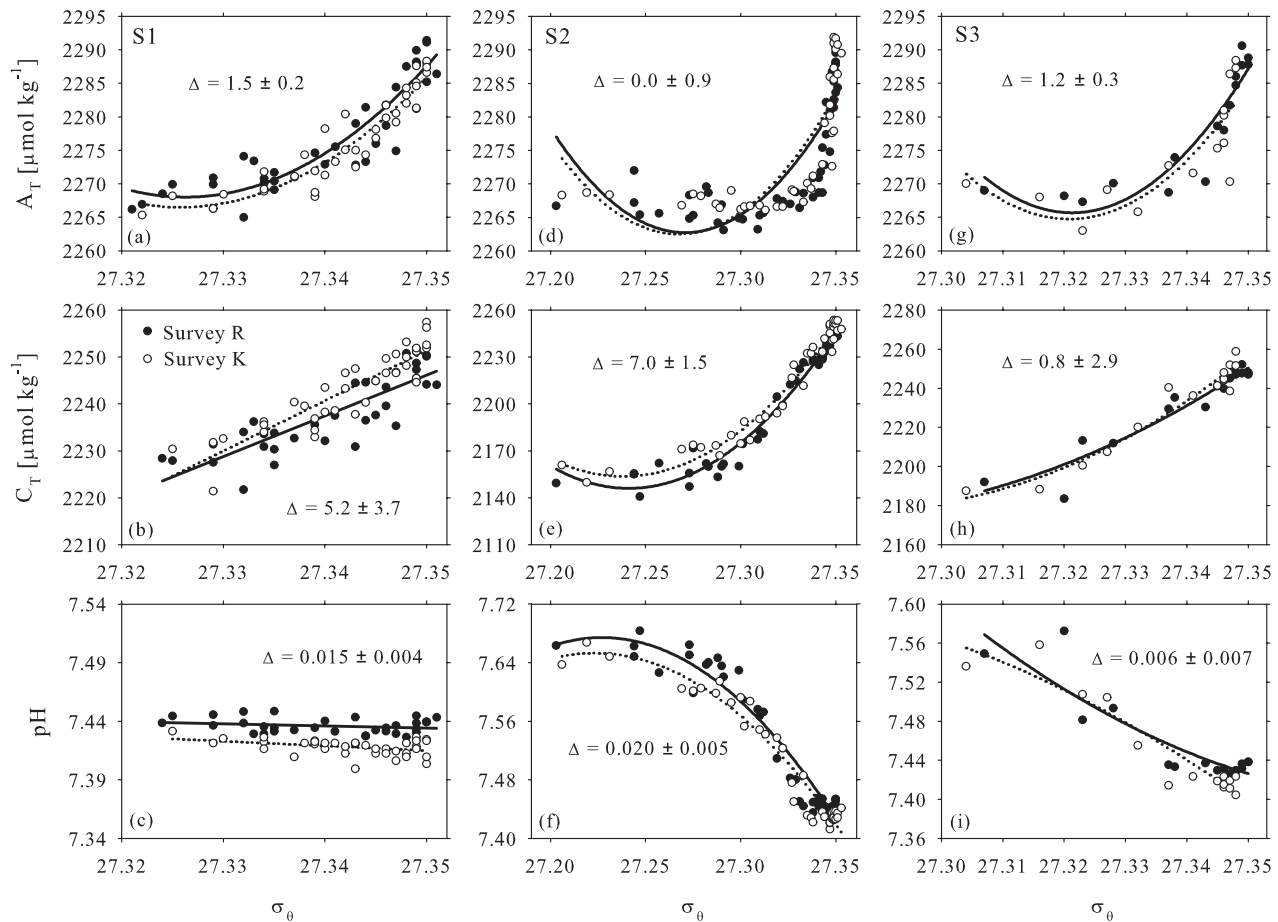
Figure 2. Comparison plots of total alkalinity (A$_T$), total dissolved inorganic carbon (C$_T$), and pH for the regions (S1−S3 in Figure 1) where the two surveys either overlap or collected data at similar locations. Data collected for Survey R are fitted to a second-order polynomial function and plotted as solid symbols (solid lines), while those collected for Survey K are also fitted to a second-order polynomial function and shown as open symbols (dotted lines). Values (Δ) in shown in the figures denote the mean differences and standard deviations (1σ) between the two curve fits.

calculated C$_T^{EQ}$ values were then linearized by a least squares linear fit, yielding the equation

$$C_T^{EQ} = 2063 - 8.753(\theta - 5) + 95.64(S - 34) \\ -1.474(A_T^o - 2270),$$ (4)

with a standard deviation (1σ) between the linearized and calculated C$_T^{EQ}$ of ±0.9 μmol kg^{-1}.

[12] The values of air-sea CO$_2$ disequilibrium (ΔC^{DISEQ}) were calculated according to the following equation:

$$\Delta C^{DISEQ} = C_T^{CAL} - \Delta C^{BIO} - C_{T}^{EQ}{}_T.$$ (5)

C$_T^{EQ}$$_T$ is the total dissolved inorganic carbon in equilibrium with the corresponding atmospheric fCO$_2$ at the time that the water parcel was at the ocean surface (sampling date − pCFC-12 age). The apparent age of the subsurface water parcel using pCFC-12 is defined as the time difference between the measurement year and the year when the water parcel was last in contact with the atmosphere. However, the

pCFC-12 water age is not necessarily identical to the true water age because of the nonlinear mixing of waters with different ages and possible undersaturation of CFC-12 at the surface when the surface water lost contact with the atmosphere during the winter [*Min and Warner*, 2005; *Matsumoto and Gruber*, 2005].

[13] Mixing between waters ventilated during the period 1960−1990 is expected to result in a relatively small age bias because pCFC-12 in the atmosphere increased approx-

Table 1. Systematic Discrepancies (Survey R−Survey K) in Parameters Recorded in Regions For Which the Two Surveys Overlap

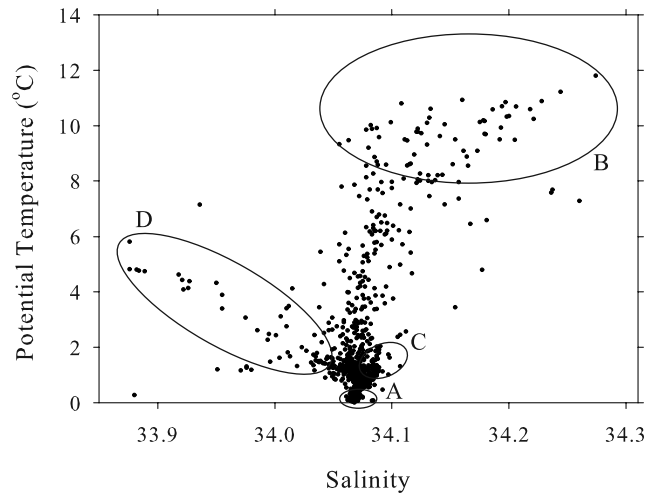| Crossovers	S	θ	O$_2$	pH	A$_T$	C$_T$
S1	0.0003	0.0068	−0.45	0.015	1.50	−5.17
S2	−0.0018	−0.0263	−1.92	0.020	0.01	−6.98
S3	−0.0004	0.0096	−1.11	0.006	1.18	−0.82
Average discrepancies	−0.0006	−0.0033	−1.16	0.014	0.90	−4.32
S.D.	0.0010	0.0199	0.74	0.007	0.78	3.17

Figure 3. Temperature-salinity diagram for all East Sea data points for which anthropogenic CO$_2$ can be estimated. Data within the four ovals were used to define the chemical properties of the four source waters (see Table 2 for a summary of results).

imately linearly during this period [*Matsumoto and Gruber*, 2005]. Therefore, in the present study we restricted the use of pCFC-12 based ages to waters younger than 40 years old. However, in the northern Japan Basin, in which the formation of deep water occurs, the surface CFC-12 concentrations observed during the winter are approximately 80% saturated with respect to atmospheric CFC-12 in 2000 [*Min and Warner*, 2005]. This 20% undersaturation of CFC-12 at the surface yielded resulting pCFC-12 water ages that are 2 to 5 years younger than those that would have resulted if the surface water had been in solubility equilibrium with respect to the overlying atmospheric pCFC-12. These pCFC-12 age biases result in a 1 to 2 μmol kg^{-1} underestimation of anthropogenic CO$_2$ concentrations. In the present study, we applied these corrections only to waters colder than 1°C because CFC-12 concentrations were only measured for surface waters colder than 1°C during the winter. This cold surface water occupies most of the interior East Sea that is deeper than 600 m and approximately 30% of all waters shallower than 600 m.

[14] The net air-sea disequilibrium value for any given seawater sample is expressed as the sum of the disequilibrium values of different water mass end-members,

$$\Delta C^{\text{DISEQ}} = \sum_{i-1}^{n} x_i \Delta C^{\text{DISEQ}-i}, \qquad (6)$$

where x_i ($\Sigma x_i = 1$) is the relative contribution of the specific source water i to the sample and $\Delta C^{\text{DISEQ}-i}$ is the unique

disequilibrium value for source water i. The OMP analysis was used to determine the net air-sea disequilibrium for a sample by more accurately estimating the relative contributions of the various source-water types contained in the sample. Source-water types are represented by unique values of measured conservative (temperature and salinity) and nonconservative (oxygen, silicate, phosphate, and nitrate concentrations) parameters. Four source-water types (A, B, C, and D) were identified from the θ−S diagram (Figure 3). Source water A includes nearly all waters deeper than 600 m. Waters deeper than 600 m consist of three different water masses: Central Water, Deep Water, and Bottom Water. We treated these as a single water mass (source water A) because their unique disequilibrium values are indistinguishable within ±3.0 μmol kg^{-1}. The mean values of the hydrographic properties and net air-sea disequilibrium for the four source-water types are summarized in Table 2.

2.4. Calculation of CaCO$_3$ Saturation State

[15] The degree of saturation of seawater with respect to aragonite and calcite is defined as the ion product of the concentrations of calcium ([Ca^{2+}]) and carbonate ions ([CO$_3^{2-}$]) at the in situ temperature, salinity, and pressure, divided by the stoichiometric solubility product ($K*sp$).

$$\Omega\text{arg} = \left[\text{Ca}^{2+}\right]\left[\text{CO}_3^{2-}\right]\Big/ K*sp-arg \qquad (7)$$

$$\Omega\text{cal} = \left[\text{Ca}^{2+}\right]\left[\text{CO}_3^{2-}\right]\Big/ K*sp-cal, \qquad (8)$$

where [Ca^{2+}] is estimated from salinity using the [Ca^{2+}]/salinity ratio of 0.00029377 [*Riley and Tongudai*, 1967], and [CO$_3^{2-}$] is calculated from A$_T$ and C$_T$ using the pressure-corrected thermodynamic constants that are consistent with the calibrated global field data [*Lee et al.*, 2000; *Millero et al.*, 2002]. These constants include the carbonic acid dissociation constants of *Mehrbach et al.* [1973] as refitted by *Dickson and Millero* [1987] and other ancillary constants as suggested by *Millero* [1995]. The effect of pressure on these dissociation constants has been estimated from partial molal volume and compressibility data [*Millero*, 1995]. The values of $K*sp$ were taken from *Mucci* [1983] at a given temperature and salinity at 1 atmosphere; the effect of pressure on $K*sp$ was also estimated from partial molal volume and compressibility data [*Millero*, 1995]. The preindustrial saturation horizons with respect to aragonite and calcite were calculated using measured A$_T$ and

Table 2. Properties of the Four Source Waters Identified in the East Sea

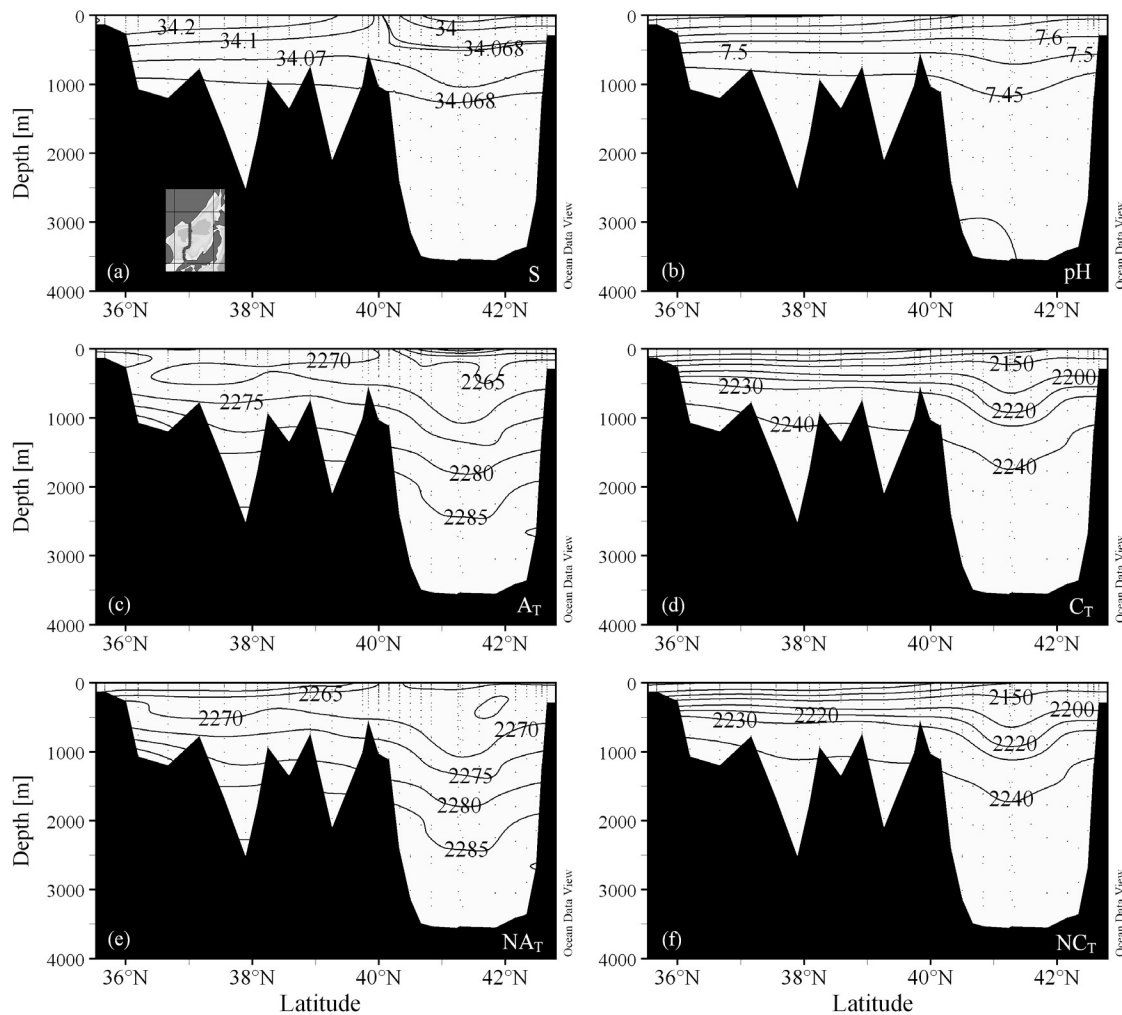| Identification	Latitude	θ	SD (θ)	S	SD (S)	O$_2$	SD (O$_2$)	PO$_4$	SD (PO$_4$)	NO$_3$	SD (NO$_3$)	Si	SD (Si)	ΔC$^{\text{DISEQ}}$	SD (ΔC$^{\text{DISEQ}}$)
A	40.30	0.18	0.12	34.07	0.01	214.72	6.90	1.99	0.06	25.12	0.62	71.06	12.79	8.84	3.02
B	38.67	9.20	0.98	34.13	0.04	260.22	5.97	0.52	0.10	6.90	1.30	8.72	2.10	−24.67	5.17
C	42.88	1.14	0.25	34.09	0.00	281.49	17.36	1.36	0.17	17.35	2.20	28.56	5.04	2.00	2.20
D	40.80	1.71	1.00	34.03	0.05	282.39	24.65	1.18	0.32	14.96	4.25	23.04	6.97	0.42	4.27

Figure 4. Meridional sections of (a) salinity, (b) pH, (c) total alkalinity (A$_T$), (d) total dissolved inorganic carbon (C$_T$), (e) salinity (S = 34.07)-normalized total alkalinity (NA$_T$ = A$_T$ × 34.07/S), and (f) salinity (S = 34.07)-normalized total dissolved inorganic carbon (NC$_T$ = C$_T$ × 34.07/S) nominally along 134°E in the East Sea. Dots indicate locations of measured data. The inset in Figure 4a shows the path of the cruise track.

preindustrial C$_T$, which was estimated by subtracting C^{ANT} from C$_T^{CAL}$.

3. Results and Discussion

3.1. Distribution of Carbon Parameters (A$_T$, C$_T$, and pH)

[16] Salinity is the dominant factor that affects A$_T$ in the surface mixed layer of the oceans [*Millero et al.*, 1998; *Lee et al.*, 2006]. The highest values of surface water A$_T$ (~2270 μmol kg^{-1}) are found in the southern East Sea (36°N−40°N) where salinity maxima as high as S > 34.2 are observed (Figure 4a). These salinity maxima extend to the subarctic polar front (near 40°N), which is formed from the interaction of subpolar water that originates from the northern part of the East Sea and subtropical water that flows into the East Sea through the Korea Strait [e.g., *Legeckis*, 1978; *Kim et al.*, 2001;

Tishchenko et al., 2003]. From the Korea Strait to the northwestern part of the East Sea, salinity and A$_T$ decrease to S = 33.0−34.0 and A$_T$ = 2250−2260 μmol kg^{-1}, respectively (Figures 4a and 4c). The surface water C$_T$ concentration is also greatly affected by factors that influence salinity, as is surface water A$_T$ [*Lee et al.*, 2000]. Biological activities also generate variations in surface water A$_T$ in the East Sea; however, the magnitude of such biologically induced changes in A$_T$ is likely to be negligible [*Kim et al.*, 2006] because calcifying organisms, which are the dominant biological contributors to A$_T$, are rarely found in the East Sea [*Kang and Choi*, 2002]. Biological activities affect C$_T$ to a significantly greater extent than they affect surface water A$_T$.

[17] The values of A$_T$ and C$_T$ (as well as NA$_T$ = A$_T$ × 34.07/S and NC$_T$ = C$_T$ × 34.07/S, S = 34.07 was chosen as the mean salinity of the East Sea) increase gradually with depth up to 2500 m and 2000 m, respectively (Figures 4c

and 4d). For waters deeper than these depths, A$_T$ and C$_T$ remain almost constant to the ocean floor. To a first order approximation, a 15 μmol kg^{-1} increase in NA$_T$ with depth is probably related to the dissolution of CaCO$_3$ particles within the water column or from sediments, whereas a 90 μmol kg^{-1} increase in NC$_T$ with depth is related to both the dissolution of CaCO$_3$ and the oxidation of organic matter (Figures 4e and 4f). Thus, given that a 15 μmol kg^{-1} increase in A$_T$ is equivalent to an increase in C$_T$ of approximately 7.5 μmol kg^{-1}, the relative contribution of organic matter and biogenic CaCO$_3$ to observed C$_T$ increase in the East Sea is approximately 11:1. This ratio of 11:1 is approximately consistent with the global rain ratio of organic matter and CaCO$_3$ at the bottom of the seasonal mixed layer [*Lee*, 2001; *Sarmiento et al.*, 2002].

[18] The pH at 25°C in the East Sea decreases from 7.92 at the surface to 7.45 at 1000 m and then remains approximately constant for deeper waters (Figure 4b). Oxidation of organic matter within the water column is the main control on the vertical distribution of pH in the East Sea. The constant pH observed throughout the water column below 1000 m suggests that negligible organic matter is present below this depth and that any decrease in pH related to the oxidation of organic matter buried in the seafloor sediment is also negligible.

3.2. Air-Sea Disequilibrium (ΔC^{DISEQ})

[19] The mean air-sea disequilibrium values for the four types of source water are summarized in Table 2. Source water A probably forms during winter cooling in regions of relatively high latitude (40°N–42°N and 132°E–133°E) near Peter the Great Bay off Vladivostok, Russia. Source water A has a positive ΔC^{DISEQ} value, suggesting that it was slightly supersaturated with respect to atmospheric fCO$_2$ when it formed at the surface during wintertime. Deep convective mixing with subsurface waters during wintertime cooling would bring deep CO$_2$-rich waters to the surface and cause the surface water fCO$_2$ value to increase above the atmospheric fCO$_2$ level. During wintertime observations of the air-sea difference of fCO$_2$ (ΔfCO$_2$ = fCO$_{2AIR}$ − fCO$_{2SEA}$) in the East Sea [*Oh et al.*, 1999; *Tishchenko et al.*, 2003], negative ΔfCO$_2$ values (which are consistent with positive ΔC^{DISEQ} values) were observed off Vladivostok in the northern part of the East Sea, where source water A probably forms. This positive ΔC^{DISEQ} value for source water A in the region of deep water formation stands in contrast to the negative ΔC^{DISEQ} value of −16 μmol kg^{-1} previously reported for North Atlantic Deep Water [*Gruber*, 1998; *Lee et al.*, 2003]. This negative value of ΔC^{DISEQ} implies that the surface waters in the deep water formation region of the North Atlantic are undersaturated with respect to atmospheric fCO$_2$.

[20] Source water B, which has a ΔC^{DISEQ} value of −25 μmol kg^{-1}, is found in the southern part of the East Sea. The negative ΔC^{DISEQ} value is explained by the following mechanism. A branch of the Tsushima warm current flows into the East Sea through the Korea Strait and then continues northward along the east coast of Korea as a western boundary current. During its northward movement, the warm water continues to interact

with cooler air and consequently cools considerably. This temperature decrease causes the fCO$_2$ of the surface water to drop below the atmospheric fCO$_2$ level, which would likely result in a negative ΔC^{DISEQ} value for source water B. Active photosynthesis also contributes to the recorded decrease in the surface water fCO$_2$ in this area [*Kim et al.*, 2001; *Gamo et al.*, 2001; *Min and Warner*, 2005]. The other two source waters, C and D, have approximately neutral ΔC^{DISEQ} values. These two source waters probably correspond to the High Salinity Intermediate Water and East Sea Intermediate Water typically found at approximately 200–300 m depth in the Japan Basin [*Kim et al.*, 2004].

3.3. Distribution of Anthropogenic CO$_2$

[21] Figures 5a and 5b show the meridional and zonal distributions of anthropogenic CO$_2$ in the East Sea. The highest concentrations of anthropogenic CO$_2$ (typically 50–60 μmol kg^{-1}) are found in the upper waters of the southern East Sea. In the southern East Sea, vertical mixing of surface waters and subsurface waters is limited by strongly developed stratification that leads to higher values of anthropogenic CO$_2$ in the upper waters. In the northern East Sea, however, surface waters mix to a great extent with old waters that contain lower concentrations of anthropogenic CO$_2$, thus lowering the anthropogenic CO$_2$ concentration of the upper waters.

[22] Anthropogenic CO$_2$ generally penetrates to the bottom of the entire basin of the East Sea, and its concentration in deep waters near the bottom reaches approximately 10–15 μmol kg^{-1}. *p*CFC-12 tracer ages of deep waters that contain 10–15 μmol kg^{-1} of anthropogenic CO$_2$ are approximately 40 years old (dotted lines in Figures 5c and 5d). There is a similarity in the meridional and zonal distributions of anthropogenic CO$_2$ concentration and *p*CFC-12 (Figures 5a–5d), because both anthropogenic gases penetrate to deep water levels via deep water formation. Deep water formation effectively transports surface waters loaded with anthropogenic gases to the interior of the basin during the winter cooling period. This transport mechanism is similar to that operating in the North Atlantic, where anthropogenic CO$_2$ reaches depths greater than 3000 m [*Lee et al.*, 2003]. In contrast, anthropogenic CO$_2$ at the same latitude in the North Pacific Ocean does not penetrate beyond 1500 m, largely due to a lack of deep water formation [*Sabine et al.*, 2002].

3.4. Inventory of Anthropogenic CO$_2$

[23] The inventory of anthropogenic CO$_2$ (TOTAL − C^{ANT}) for each 2.5° latitude × 2.5° longitude grid element was determined by integrating the area-weighted mean profile of C^{ANT} (f − C^{ANT}) from the surface (SFC) to the mean bottom depth (MEAN),

$$\text{TOTAL} - \text{C}^{ANT} = \int_{\text{SFC}}^{\text{MEAN}} A\, f - \text{C}^{ANT} dz, \qquad (9)$$

where A (m^2) is the area of each 2.5° latitude × 2.5° longitude grid element. The estimated inventories for each
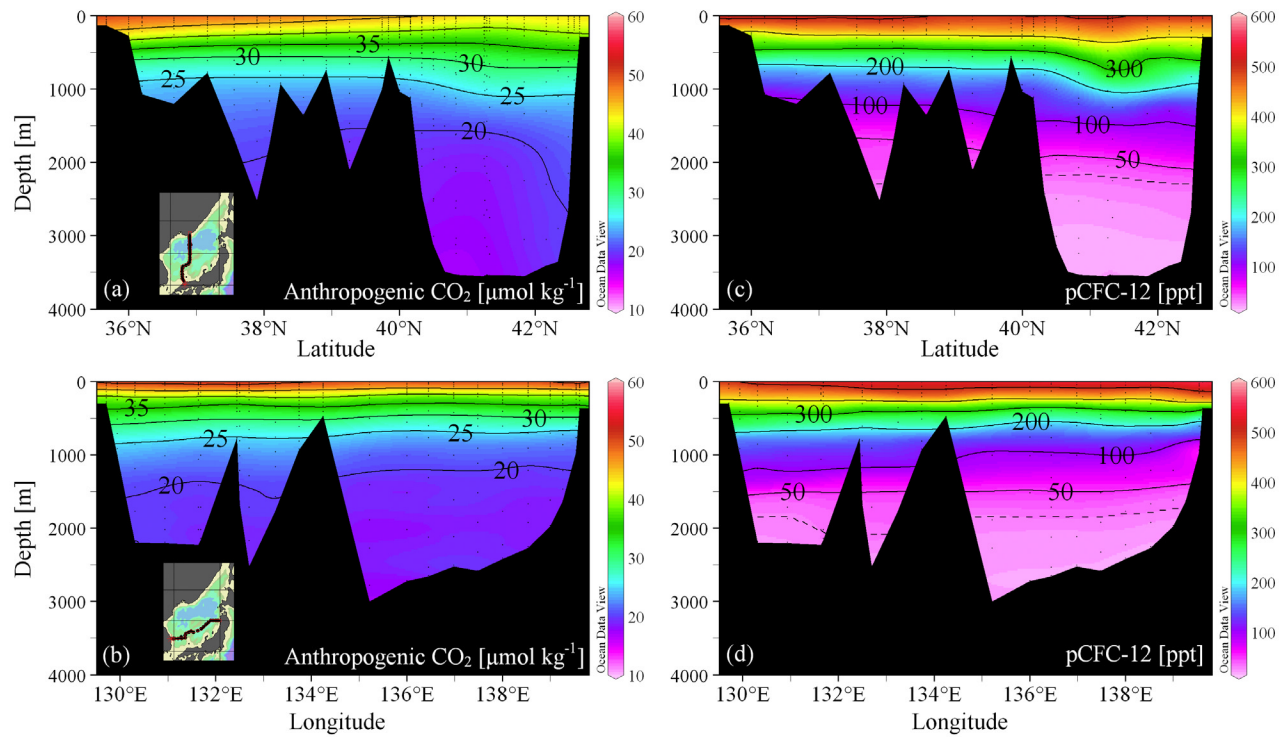
Figure 5. (a, c) Meridional and (b, d) zonal sections of anthropogenic CO$_2$ and pCFC-12 nominally along 134°E and 38°N in the East Sea, respectively. Deep waters near the bottom (~3500 m depth) of the Japan Basin contain approximately $10-15$ μmol kg^{-1} of anthropogenic CO$_2$. Dotted lines represent water masses of approximately 40 years in age. Anthropogenic CO$_2$ concentrations are not scaled down because corrections for the key systematic errors (inaccuracies in the assumption of the constant air-sea disequilibrium and the pCFC-12 age bias) differ for different water masses.

of the grid elements were then summed to produce the basin-wide inventory of anthropogenic CO$_2$. The total amount of anthropogenic CO$_2$ that has accumulated in the East Sea between 1800 and 1999 is equal to 0.51 petagrams of carbon (Pg C, Pg = 10^{15} g), which is just 0.01 Pg C more than the inventory obtained without correction for pCFC-12 age bias related to the 20% undersaturation of CFC-12 observed in the wintertime outcrop regions.

[24] The highest specific column inventory (TOTAL − C^{ANT} divided by the area of each 2.5° latitude × 2.5° longitude grid element; moles of anthropogenic CO$_2$ per m^2) is observed in the Japan Basin between 40°N and 44°N, and between 131°E and 139°E, with a mean value of 80 mol C m^{-2} (Figure 6). This figure is much higher than the $20-30$ mol C m^{-2} observed in the adjacent North Pacific [*Sabine et al.*, 2002]. The high specific column inventory in the East Sea compared to that at the same latitude band in the North Pacific can be attributed to the sinking of newly formed water into the interior that contains significant quantities of anthropogenic CO$_2$. Such deep water formation was observed south of Vladivostok in the cold winter of 2001 [*Kim et al.*, 2002; *Talley et al.*, 2003]. Brine rejection into adjacent waters during the formation of sea ice resulted in dense surface waters that subsequently sank into the interior of the basin [*Talley et al.*, 2003]. Within the Japan Basin, the specific column inventories in the central and western areas are lower than those in the

eastern area despite the fact that the deep water formation process is more active in the central and western parts of the Japan Basin. This pattern is directly attributable to the lower volumes of waters in the central and western basins compared to the eastern basin.

[25] We identified two key sources of systematic errors that could potentially have biased our estimation of anthropogenic CO$_2$ inventory. The first source of error arises from inaccuracies in the assumed value of the constant air-sea disequilibrium used in the ΔC* approach. This bias results in an overestimation of anthropogenic CO$_2$ in the younger waters that occupy much of the interior of the East Sea. We correct for this bias in the East Sea using the procedure proposed by *Matsumoto and Gruber* [2005], whereby the anthropogenic CO$_2$ inventory of 0.51 Pg C should be scaled down by approximately 14%. The second source of error is a pCFC-12 age bias related to the nonlinear mixing of waters of different ages. Although it is not possible to estimate the exact magnitude of this error, various modeling studies indicate that pCFC-12 based ages are $5-10$ years younger than true ages, with the magnitude of the age bias being dependent on the degree of mixing in the interior [*Matsumoto and Gruber*, 2005; *Hall et al.*, 2002, 2004; *Waugh et al.*, 2004]. If this age bias is properly corrected, the revised inventory should be scaled down by approximately 8%. Considering these two corrections together, the inventory should be scaled down to as low as 0.40 Pg.
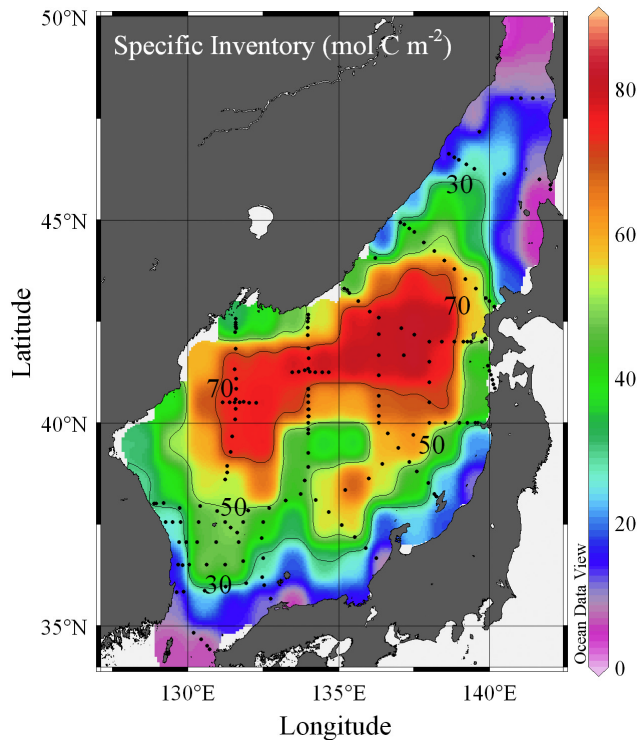
Figure 6. Map of anthropogenic CO_2 column inventory (mol C m^{-2}) in the East Sea. The anthropogenic CO_2 inventory for waters in the northwestern East Sea near North Korea was estimated by extrapolating anthropogenic CO_2 concentrations from adjacent waters. Anthropogenic CO_2 column inventory are not scaled down because corrections for the key systematic errors (inaccuracies in the assumption of the constant air-sea disequilibrium and the pCFC-12 age bias) differ for different water masses. Circles represent sampling locations of Surveys K and R.

[26] There are two additional sources of errors: uncertainty in the precision of various measurements required for the calculation of anthropogenic CO_2, and uncertainties in the end-member disequilibrium values. The propagation of measurement errors indicates that any anthropogenic CO_2 estimate in the East Sea has an uncertainty of ±7.3 μmol kg^{-1}; however, this random error should largely cancel out. Approximate upper (or lower) estimates of ΔC^{DISEQ} for each data point were calculated by increasing (or decreasing) the mean ΔC^{DISEQ} value by the standard deviation of the mean value for each source-water type. This analysis yielded an error of ±0.06 Pg C in anthropogenic CO_2 inventory. *Lee et al.* [2003] applied this error estimation method to the Atlantic Ocean.

3.5. Uptake of Anthropogenic CO₂ Over the Period 1992 to 1999

[27] In conjunction with anthropogenic CO_2 results presented in this paper, results estimated from the A_T and C_T data sets collected during the Kuroshio Edge Exchange Processes-Marginal Sea Studies Expedition in the East Sea (July 28 to August 5, 1992) [*Chen et al.*, 1995] provide

an opportunity to calculate the increase of anthropogenic CO_2 inventory over the 7-year period from 1992 to 1999. We used the isopycnal method to calculate the total anthropogenic CO_2 that accumulated in the East Sea over the 7-year period. This method was used previously to determine decadal rates of anthropogenic CO_2 uptake in the Indian and Pacific Oceans [*Peng et al.*, 1998, 2003]. The method directly compares C_T values measured at the same geographic location at two different times after correcting for CO_2 changes related to the oxidation of organic matter, dissolution of calcium carbonate, and variations in salinity. The net increase in corrected C_T at a selected isopycnal surface is assumed to represent the amount of anthropogenic CO_2 taken up during the time interval between the two different measurement dates.

[28] We only determined the anthropogenic CO_2 taken up by the East Sea and stored for the 7-year period for the Japan Basin owing to a lack of inorganic carbon data collected during the 1992 cruise. In comparing the 1992 and 1999 data, we found that the 1992 data contains systematic errors of 21 μmol kg^{-1} in A_T, 13 μmol kg^{-1} in C_T, and 6.5 μmol kg^{-1} in O_2. We then applied these discrepancies to the 1992 data. To avoid seasonal variations in C_T in the upper ocean, data collected for waters shallower than 300 m were not used in this calculation. We estimated the 7-year uptake rate of anthropogenic CO_2 for isopycnal surfaces, the potential densities of which range from $\sigma\theta$ = 27.320 to 27.345. This density range corresponds approximately to a depth range of 400−1300 m. The total inventory of anthropogenic CO_2 accumulated in the East Sea during this 7-year period was estimated by integrating the profile of anthropogenic CO_2 concentration from the surface to a depth of 1300 m (Figure 7); the resulting mean inventory is approximately 4.6 ± 2.7 mol m^{-2}, which yields a mean annual uptake rate of 0.66 ± 0.38 mol m^{-2} yr^{-1}. The large degree of uncertainty associated with this estimate of annual uptake rate is primarily due to the lack of inorganic carbon data collected during the 1992 cruise.

[29] Our estimate of the accumulation rate of anthropogenic CO_2 in the Japan Basin is similar to that obtained for
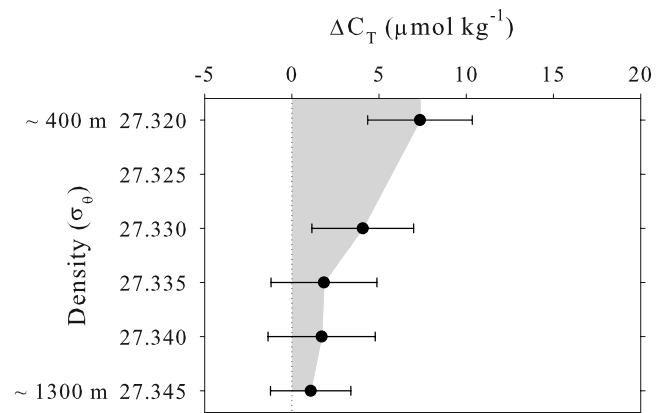

Figure 7. Mean differences in C_T concentrations between the 1992 and 1999 data sets as a function of density surface. Error bars represent 1 standard deviation from the mean.
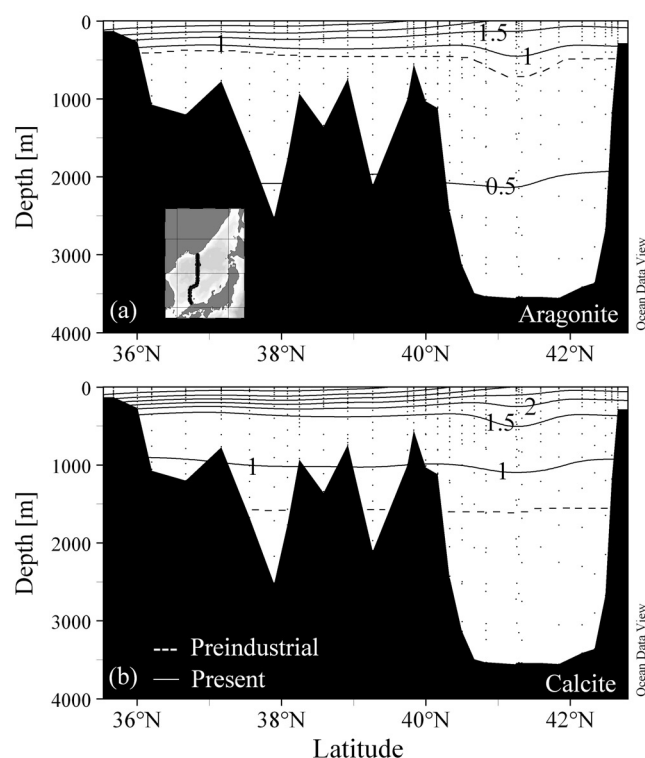
Figure 8. Meridional distributions of the degree of seawater saturation with respect to (a) aragonite and (b) calcite at the present day (solid lines), nominally along 134°E in the East Sea. The dotted lines denote the aragonite and calcite saturation horizons ($\Omega = 1$) during the preindustrial era. The inset in Figure 8a shows the path of the cruise track.

the northeast Pacific using the same isopycnal method [*Peng et al.*, 2003], despite the much higher specific column inventory recorded in the East Sea compared to the North Pacific. This similarity probably reflects a weakening of deep water formation in the East Sea during the 1990s. Several previous studies suggest that deep water formation in the East Sea has weakened over the past several decades, resulting in outcrop waters being fed into the intermediate layer rather than the deep layer [*Kim and Kim*, 1996; *Gamo et al.*, 2001; *Kim et al.*, 2001, 1999, 2002; *Talley et al.*, 2003]. This weakening, which has been attributed to global warming [*Kim and Kim*, 1996; *Gamo et al.*, 2001], could lead to reduced efficiency in the transport of anthropogenic CO₂ to the interior of the East Sea. A similar decrease in the intensity of bottom water formation has also been observed for the North Atlantic Ocean [*Wood et al.*, 1999; *Hansen et al.*, 2001]. Such variations in the intensity of deep water formation and turnover time could potentially affect the sequestration of anthropogenic CO₂ by the oceans.

3.6. Comparisons With Other Marginal Seas

[30] Deep water formation occurs in various marginal seas, including the Arctic Ocean, East Sea, Labrador Sea, Mediterranean Sea, Okhotsk Sea, and Weddell Sea. Of these, the Sea of Okhotsk is a subpolar marginal sea located

northeast of the East Sea and contains the southernmost region of sea ice in the Northern Hemisphere. In the Okhotsk Sea, dense water produced as a result of brine rejection during the formation of sea ice is fed into the intermediate layer of the North Pacific [e.g., *Talley*, 1991; *Yasuda*, 1997; *Shcherbina et al.*, 2003]. This dense water carries some of the anthropogenic CO₂ taken up by the surface of the Okhotsk Sea. In contrast, there is only a limited exchange of waters between the East Sea and the North Pacific; hence, CO₂ taken up by the surface of the East Sea continuously accumulates at that site. These differences in deep water circulation patterns are the likely explanation for the fact that the annual accumulation rate of anthropogenic CO₂ in the Okhotsk Sea, which has been estimated to be 0.78×10^{-3} Pg C yr^{-1} [*Wakita et al.*, 2003], is significantly lower than the rate of 1.6×10^{-3} Pg C yr^{-1} recorded in the East Sea.

[31] In contrast, deep water formation in the abyssal Weddell Sea is believed to be less important with respect to the accumulation rate of anthropogenic CO₂ [*Hoppema et al.*, 2001; *Poisson and Chen*, 1987]. The concentration of anthropogenic CO₂ in the Weddell Sea falls sharply below 5 μmol kg^{-1} at a depth of about 500 m [*Hoppema et al.*, 2001]. The shallower penetration and lower inventory of anthropogenic CO₂ in this sea is attributed to various factors. One of these factors is the limited exchange of CO₂ at the air-sea interface because of the fact that sea-ice covers the surface for much of the year, inhibiting air-sea CO₂ exchange and allowing only a short residence time for newly formed deep waters to absorb anthropogenic CO₂ from the atmosphere [*Caldeira and Duffy*, 2000; *Hoppema et al.*, 2001]. A second factor is the significant dilution of anthropogenic CO₂ by mixing with old Weddell Deep Water, which is poor in anthropogenic CO₂ [*Poisson and Chen*, 1987; *Hoppema et al.*, 2001].

[32] Until recently, the Arctic Ocean was believed to be an insignificant sink of anthropogenic CO₂ because much of the basin surface is covered with sea ice. However, a recent man-made tracer-based modeling study [*Anderson et al.*, 1998] indicated the active ventilation of intermediate water in the Arctic Ocean, through which a considerable amount of anthropogenic CO₂ is believed to be absorbed. On the basis of the results of this previous study, the mean inventory of anthropogenic CO₂ per unit area of the Arctic Ocean in the 1990s was estimated to be approximately 360 g C m^{-2} [*Anderson et al.*, 1998], which is similar to the value of 400 g C m^{-2} determined for the East Sea.

3.7. Upward Displacement of the Aragonite and Calcite Saturation Horizons

[33] Because some of the protons generated from the dissolution of anthropogenic CO₂ in seawater react with carbonate ions to form bicarbonate ions, the invasion of anthropogenic CO₂ into the ocean results in a decrease in the concentration of carbonate ion, which in turn acts to reduce the saturation states of seawater with respect to aragonite and calcite. The saturation horizons ($\Omega = 1$) for aragonite and calcite in the East Sea for both present (solid lines) and preindustrial (dotted lines) levels are shown in Figure 8. The degree of saturation decreases

with depth because the solubility of aragonite and calcite generally increases with depth [*Mucci*, 1983]. The present-day saturation horizons of aragonite and calcite in the East Sea are located at depths of approximately 400 m and 1000 m, respectively. The depth of the aragonite saturation horizon in the East Sea is similar to that in the adjacent Pacific Ocean [*Feely et al.*, 2002]. In contrast, the saturation horizon for calcite is approximately 300−600 m deeper in the East Sea than that at the same latitude band in the North Pacific.

[34] Since the preindustrial era, the saturation horizons for aragonite and calcite in the East Sea have moved upward by approximately 80−220 m and 500−700 m, respectively, across the entire basin (Figure 8). These upward migrations of the saturation horizons are significantly greater than those observed for the same latitude band of the North Pacific (i.e., 40−50 m for aragonite and 100−150 m for calcite) [*Feely et al.*, 2002, 2004]. The greater upward shift of the saturation horizons in the East Sea compared to the North Pacific can be attributed to two main factors: the deeper penetration of anthropogenic CO$_2$ in the East Sea, and a significantly smaller vertical gradient in the degree of aragonite and calcite saturation in the East Sea. The interior of the East Sea at depths greater than 800 m has almost uniform aragonite and calcite saturation states throughout, with variation in the aragonite saturation state between 1000 m and 3500 m depth of slightly more than $\Omega = 0.5$ and equivalent variation for calcite of $\Omega = 0.5$. As a result, a given amount of anthropogenic CO$_2$ will have a more profoundly affect on the aragonite and calcite saturation states in the East Sea than on those in the North Pacific. In the North Pacific, there is a significant vertical gradient in the degree of saturation of seawater with aragonite and calcite. Taken together, the above factors cause the aragonite and calcite saturation horizons in the East Sea to migrate upward to a significantly greater extent than those observed in other major basins of the global ocean.

4. Conclusions

[35] In this study, we estimated the anthropogenic CO$_2$ inventory in the East Sea using a high-quality inorganic carbon data set collected during a comprehensive survey conducted in the summer of 1999. The distribution of anthropogenic CO$_2$ in the East Sea shows features that are consistent with the distributions found in other major basins within which deep water formation occurs (e.g., the North Atlantic); most notably, high column inventories of anthropogenic CO$_2$ were observed in the region of deep water formation near Peter the Great Bay off Vladivostok, Russia. The deep water formation process effectively carries anthropogenic CO$_2$ into the interior of the East Sea. In particular, the specific column inventory of anthropogenic CO$_2$ in the East Sea is two to three times greater than that in the North Pacific, in which only intermediate water formation occurs.

[36] The substantial accumulation of anthropogenic CO$_2$ in the East Sea has caused a significant change in the carbonate chemistry of the sea. In particular, the anthropogenic CO$_2$-induced upward movement of the saturation

horizons for aragonite and calcite is significantly greater in the East Sea than in other major basins. This notable change in carbonate chemistry is likely driven by two unique characteristics of the East Sea: a fast turnover time (<100 years), which is directly related to active deep water formation; and a small dynamic range of temperature and salinity, which is one to two orders of magnitude smaller than the ranges found in the major oceans. This small degree of vertical variability suggests that the water column in the East Sea is relatively unstable. As a result, minor disturbances in the global or regional climate system will potentially change the intensity of deep water formation [*Kim and Kim*, 1996], which directly affects the uptake of anthropogenic CO$_2$ by the East Sea. Regular monitoring of carbon and hydrographic parameters in the East Sea will therefore provide information on variations that may occur in the global ocean at much longer time scales. In this way, the East Sea can serve as a site for monitoring decadal variability in oceanic CO$_2$ uptake.

References

Anderson, L. A., and J. L. Sarmiento (1994), Redfield ratios of remineralization determined by nutrient data analysis, *Global Biogeochem. Cycles*, *8*, 65–80.

Anderson, L. G., K. Olsson, E. P. Jones, M. Chierici, and A. Fransson (1998), Anthropogenic carbon dioxide in the Arctic Ocean: Inventory and sinks, *J. Geophys. Res.*, *103*, 27,707–27,716.

Broecker, W. S. (1974), 'NO', a conservative water-mass tracer, *Earth Planet. Sci. Lett.*, *23*, 100–107.

Bruevich, S. V. (1944), Determination of alkalinity in small volumes of seawater by direct titration, in *Instruction of Chemical Examination of Seawater*, p. 83, Glavsevmorput, Moscow.

Caldeira, K., and P. B. Duffy (2000), The role of the Southern Ocean in uptake and storage of anthropogenic carbon dioxide, *Science*, *287*, 620–622.

Chen, C.-T. A., S.-L. Wang, and A. S. Bychkov (1995), Carbonate chemistry of the Sea of Japan, *J. Geophys. Res.*, *100*, 13,737–13,745.

Dickson, A. G. (1984), pH scales and proton-transfer reactions in proton-transfer reactions in saline media such as seawater, *Geochim. Cosmochim. Acta*, *48*, 2299–2308.

Dickson, A. G., and F. J. Millero (1987), A comparison of the equilibrium constants for the dissociation of carbonic acid in seawater media, *Deep Sea Res., Part I*, *34*, 1733–1743.

Dickson, A. G., and J. P. Riley (1979), The estimation of acid dissociation constants in seawater from potentiometric titrations with strong base: II. The dissociation of phosphoric acid, *Mar. Chem.*, *7*, 101–109.

Feely, R. A., et al. (2002), In situ calcium carbonate dissolution in the Pacific Ocean, *Global Biogeochem. Cycles*, *16*(4), 1144, doi:10.1029/2002GB001866.

Feely, R. A., C. L. Sabine, K. Lee, W. Berelson, J. Kleypas, V. J. Fabry, and F. J. Millero (2004), Impact of anthropogenic CO$_2$ on the CaCO$_3$ system in the oceans, *Science*, *305*, 362–366.

Gamo, T., N. Momoshima, and S. Tolmachyov (2001), Recent upward shift of the deep convection system in the Japan Sea, as inferred from the geochemical tracers tritium, oxygen, and nutrients, *Geophys. Res. Lett.*, *28*, 4143–4146.

Gruber, N. (1998), Anthropogenic CO$_2$ in the Atlantic Ocean, *Global Biogeochem. Cycles*, *12*, 165–191.

Gruber, N., J. L. Sarmiento, and T. F. Stocker (1996), An improved method for detecting anthropogenic CO$_2$ in the oceans, *Global Biogeochem. Cycles*, *10*, 809–837.

Hall, T. M., T. W. N. Haine, and D. W. Waugh (2002), Inferring the concentration of anthropogenic carbon in the ocean from tracers, *Global Biogeochem. Cycles*, *16*(4), 1131, doi:10.1029/2001GB001835.

Hall, T. M., D. W. Waugh, T. W. N. Haine, P. E. Robbins, and S. Khatiwala (2004), Estimates of anthropogenic carbon in the Indian Ocean with allowance for mixing and time-varying air-sea CO$_2$ disequilibrium, *Global Biogeochem. Cycles*, *18*, GB1031, doi:10.1029/2003GB002120.

Hansen, B., W. R. Turrell, and S. Osterhus (2001), Decreasing overflow from the Nordic seas into the Atlantic Ocean through the Faroe Bank channel since 1950, *Nature*, *411*, 927–930.

Hansson, I. (1973), A new set of pH-scales and standard buffers for seawater, *Deep Sea Res.*, *20*, 479–491.

Hoppema, M., W. Roether, R. G. J. Bellerby, and H. J. W. d. Baar (2001), Direct measurements reveal insignificant storage of anthropogenic CO$_2$ in the abyssal Weddell Sea, *Geophys. Res. Lett.*, *28*, 1747–1750.

Kang, Y. S., and J. K. Choi (2002), Ecological characteristics of phytoplankton communities in the coastal waters of Gori, Wolseong, Uljin and Younggwang II. Distributions of standing crops and environmental variables (1992–1996) (in Korean), *J. Kor Soc. Oceanogr.*, *7*, 108–128.

Kawamura, H., and P. Wu (1998), Formation mechanism of Japan Sea Proper Water in the flux center off Vladivostok, *J. Geophys. Res.*, *103*, 21,611–21,622.

Kim, H.-C., K. Lee, and W. Choi (2006), Contribution of phytoplankton and bacterial cells to the measured alkalinity of seawater, *Limnol. Oceanogr*, *51*, 331–338.

Kim, K., et al. (1996), New finding from CREAMS observations: Water masses and eddies in the East Sea, *J. Kor. Soc. Oceanogr.*, *31*, 155–163.

Kim, K., K.-R. Kim, D.-H. Min, Y. Volkov, J.-H. Yoon, and M. Takematsu (2001), Warming and structural changes in the East (Japan) Sea: A clue to future changes in global oceans?, *Geophys. Res. Lett.*, *28*, 3293–3296.

Kim, K., K.-R. Kim, Y.-G. Kim, Y.-K. Cho, D.-J. Kang, M. Takematsu, and Y. Volkov (2004), Water masses and decadal variability in the East Sea (Sea of Japan), *Prog. Oceanogr.*, *61*, 157–174.

Kim, K.-R., and K. Kim (1996), What is happening in the East Sea (Japan Sea)?: Recent chemical observations during CREAMS 93–96, *J. Kor. Soc. Oceanogr.*, *31*, 164–172.

Kim, K.-R., K. Kim, D.-J. Kang, S. Y. Park, M.-K. Park, Y.-G. Kim, H. S. Min, and D. Min (1999), The East Sea (Japan Sea) in change: A story of dissolved oxygen, *Mar. Technol. Soc. J.*, *33*, 15–22.

Kim, K.-R., G. Kim, K. Kim, V. Lobanov, V. Ponomarev, and A. Salyuk (2002), A sudden bottom-water formation during the severe winter 2000–2001: The case of the East/Japan Sea, *Geophys. Res. Lett.*, *29*(8), 1234, doi:10.1029/2001GL014498.

Lamb, M. F., et al. (2002), Consistency and synthesis of Pacific Ocean CO$_2$ survey data, *Deep Sea Res., Part II*, *49*, 21–58.

Lee, K. (2001), Global net community production estimated from annual cycle of surface water total dissolved inorganic carbon, *Limnol. Oceanogr.*, *46*, 1287–1297.

Lee, K., F. J. Millero, R. H. Byrne, R. A. Feely, and R. H. Wanninkhof (2000), The recommended dissociation constants of carbonic acid for use in seawater, *Geophys. Res. Lett.*, *27*, 229–232.

Lee, K., et al. (2003), An updated anthropogenic CO$_2$ inventory in the Atlantic Ocean, *Global Biogeochem. Cycles*, *17*(4), 1116, doi:10.1029/2003GB002067.

Lee, K., et al. (2006), Global relationships of total alkalinity with salinity and temperature in surface waters of the world's oceans, *Geophys. Res. Lett.*, *33*, L19605, doi:10.1029/2006GL027207.

Legeckis, R. (1978), A survey of worldwide sea surface temperature fronts detected by environmental satellites, *J. Geophys. Res.*, *83*, 4501–4512.

Matsumoto, K., and N. Gruber (2005), How accurate is the estimation of anthropogenic carbon in the ocean? An evaluation of the ΔC* method, *Global Biogeochem. Cycles*, *19*, GB3014, doi:10.1029/2004GB002397.

Mehrbach, C., C. H. Culberson, J. E. Hawley, and R. M. Pytkowicz (1973), Measurement of the apparent dissociation constants of carbonic acid in seawater at atmospheric pressure, *Limnol. Oceanogr.*, *18*, 897–907.

Millero, F. J. (1995), Thermodynamics of the carbon dioxide system in the oceans, *Geochim. Cosmochim. Acta*, *59*, 661–677.

Millero, F. J., K. Lee, and M. Roche (1998), Distribution of alkalinity in the surface waters of the major oceans, *Mar. Chem.*, *60*, 111–130.

Millero, F. J., D. Pierrot, K. Lee, R. Wanninkhof, R. A. Feely, C. L. Sabine, R. M. Key, and T. Takahashi (2002), Dissociation constants for carbonic acid determined from field measurements, *Deep Sea Res., Part I*, *49*, 1705–1723.

Min, D.-H., and M. J. Warner (2005), Basin-wide circulation and ventilation study in the East Sea (Sea of Japan) using chlorofluorocarbon tracers, *Deep Sea Res., Part II*, *52*, 1580–1616.

Mucci, A. (1983), The solubility of calcite and aragonite in seawater at various salinities, temperatures and 1 atmosphere total pressure, *Am. J. Sci.*, *238*, 780–799.

Oh, D.-C., M.-K. Park, S.-H. Choi, D.-J. Kang, S. Y. Park, J. S. Hwang, A. Andreev, G. H. Hong, and K.-R. Kim (1999), The air-sea exchange of CO$_2$ in the East Sea (Japan Sea), *J. Oceanogr.*, *55*, 157–169.

Peng, T.-H., R. Wanninkhof, J. L. Bullister, R. A. Feely, and T. Takahashi (1998), Quantification of decadal anthropogenic CO$_2$ uptake in the ocean based on dissolved inorganic carbon measurements, *Nature*, *396*, 560–563.

Peng, T.-H., R. Wanninkhof, and R. A. Feely (2003), Increase of anthropogenic CO$_2$ in the Pacific Ocean over the last two decades, *Deep Sea Res., Part II*, *50*, 3065–3082.

Poisson, A., and C.-T. A. Chen (1987), Why is there little anthropogenic CO$_2$ in the Antarctic Bottom Water?, *Deep Sea Res., Part A*, *34*, 1255–1275.

Riley, J. P., and M. Tongudai (1967), the major cation/chlorinity ratios in sea water, *Chem. Geol.*, *2*, 263–269.

Sabine, C. L., et al. (2002), Distribution of anthropogenic CO$_2$ in the Pacific Ocean, *Global Biogeochem. Cycles*, *16*(4), 1083, doi:10.1029/2001GB001639.

Sabine, C. L., R. M. Key, A. Kortzinger, R. A. Feely, R. Wanninkhof, F. J. Millero, T.-H. Peng, J. L. Bullister, and K. Lee (2005), Global ocean data analysis project (GLODAP): Results and data, *ORNL/CDIAC-145*, Carbon Dioxide Inf. Anal. Cent., Oak Ridge Natl. Lab., U.S. Dept. of Energy, Oak Ridge, Tenn.

Sarmiento, J. L., J. Dunne, A. Gnanadesikan, R. M. Key, K. Matsumoto, and R. Slater (2002), A new estimate of the CaCO$_3$ to organic carbon export ratio, *Global Biogeochem. Cycles*, *16*(4), 1107, doi:10.1029/2002GB001919.

Senjyu, T., and H. Sudo (1993), Water characteristics and circulation of the upper portion of the Japan Sea proper water, *J. Mar. Syst.*, *4*, 349–362.

Shcherbina, A. Y., L. D. Talley, and D. L. Rudnick (2003), Direct observations of North Pacific ventilation: Brine rejection in the Okhotsk Sea, *Science*, *302*, 1952–1955.

Talley, L. D. (1991), An Okhotsk Sea water anomaly: Implications for sub-thermocline ventilation in the North Pacific, *Deep Sea Res., Part A*, *38*, S171–S190.

Talley, L. D., V. Lobanov, V. Ponomarev, A. Salyuk, P. Tishchenko, and I. Zhabin (2003), Deep convection and brine rejection in the Japan Sea, *Geophys. Res. Lett.*, *30*(4), 1159, doi:10.1029/2002GL016451.

Talley, L. D., P. Tishchenko, V. Luchin, A. Nedashkovskiy, S. Sagalaev, D.-J. Kang, M. Warner, and D.-H. Min (2004), Atlas of Japan (East) Sea hydrographic properties in summer, 1999, *Prog. Oceanogr.*, *61*, 277–348.

Thomas, H., Y. Bozec, K. Elkalay, and H. J. W. de Baar (2004), Enhanced open ocean storage of CO$_2$ from shelf sea pumping, *Science*, *304*, 1005–1008.

Tishchenko, P. Y., C. S. Wong, G. Y. Pavlova, W. K. Johnson, D.-J. Kang, and K.-R. Kim (2001), The measurements of pH values in seawater using a cell without a liquid junction, *Oceanology*, *41*, 813–822.

Tishchenko, P. Y., et al. (2003), Seasonal variability of the hydrochemical conditions in the Sea of Japan, *Oceanology*, *43*, 643–655.

Tsunogai, S., S. Watanabe, and T. Sato (1999), Is there a "continental shelf pump" for the absorption atmospheric CO$_2$?, *Tellus, Ser. B*, *51*, 701–712.

Uda, M. (1934), The results of simultaneous oceanographical investigations in the Japan Sea and its adjacent waters in May and June, 1932 (in Japanese), *J. Imp. Fish. Exp. Stn.*, *5*, 57–190.

Wakita, M., Y. W. Watanabe, S. Watanabe, S. Noriki, and M. Wakatsuchi (2003), Oceanic uptake rate of anthropogenic CO$_2$ in a subpolar marginal sea: The Sea of Okhotsk, *Geophys. Res. Lett.*, *30*(24), 2252, doi:10.1029/2003GL018057.

Waugh, D. W., T. W. N. Haine, and T. M. Hall (2004), Transport times and anthropogenic carbon in the subpolar North Atlantic Ocean, *Deep Sea Res., Part I*, *51*, 1475–1491.

Wood, R. A., A. B. Keen, J. F. B. Mitchell, and J. M. Gregory (1999), Changing spatial structure of the thermocline circulation in response to atmospheric CO$_2$ forcing in a climate model, *Nature*, *399*, 572–575.

Yasuda, I. (1997), The origin of the North Pacific Intermediate Water, *J. Geophys. Res.*, *102*, 893–909.

_____

D.-J. Kang and K.-R. Kim, Research Institute of Oceanography, School of Earth and Environmental Sciences (BK21), Seoul National University, Seoul, 151-742, South Korea.

K. Lee (corresponding author) and G.-H. Park, School of Environmental Science and Engineering, Pohang University of Science and Technology, San 31, Hyoja-dong, Nam-gu, Pohang, 790-784, Korea. (ktl@postech.ac.kr)

D.-H. Min, Marine Science Institute, University of Texas at Austin, Port Aransas, TX 78373, USA.

L. D. Talley, Scripps Institution of Oceanography, University of California, San Diego, La Jolla, CA 92037, USA.

P. Tishchenko, Pacific Oceanological Institute, Far East Division, Russian Academy of Sciences, Vladivostok, 690041 Russia.

M. J. Warner, School of Oceanography, University of Washington, Seattle, WA 98195, USA.